TENSILE AND NONDESTRUCTIVE TESTING OF FRP BARS[a]

By Protasio F. Castro[1] and Nicholas J. Carino,[2] Members, ASCE

ABSTRACT: An exploratory study was carried out to support the development of standard test methods for fiber reinforced plastic (FRP) bars for use as concrete reinforcement. The principal objectives were to develop a simple, economical, and effective system to permit tensile loading of the bars in a universal test machine; to evaluate the influence of the free-length-to-bar-diameter ratio on the measured tensile strength; and to explore the potential of measuring the elastic modulus using available nondestructive test methods. A successful system for applying tensile load was developed. The ends of a bar were embedded in steel tubes using a high-strength gypsum cement mortar. The bars were loaded by gripping the tubes in the conventional wedge friction grips of a tensile testing machine. No statistically significant influence of the free-length-to-diameter ratio was observed for ratios varying between 40 and 70. However, large within-test variability of tensile strength was observed. Dynamic modulus of elasticity was determined using two stress-wave propagation methods: ultrasonic pulse velocity and resonant frequency. The dynamic values compared favorably with static values obtained from tensile stress-strain curves. Recommendations are provided for additional studies to support the development of standard test methods.

INTRODUCTION

Fiber reinforced plastic (FRP) composites in the shapes of bars are available as alternatives to steel bars for reinforcing concrete. Compared with steel, FRP bars offer the advantages of reduced mass, high tensile strength, and absence of rusting in the presence of chloride ions or carbonated concrete. On the other hand, there are significant barriers to their widespread use:

- The stress-strain behavior approximates that of a linear-elastic brittle material; this makes current design equations, based on the elastic-plastic behavior of steel, questionable. As a result, new design methods are needed to ensure the safety and serviceability of members reinforced with FRP bars.
- The brittleness of FRP bars makes it impossible to bend them after they have been manufactured.
- The elastic modulus is lower than that of steel, which may lead to large service load deflections and crack widths in flexural members.
- The lack of standard specifications and test methods makes it difficult for engineers to specify FRP bars in project documents.

FRP bars are composed of continuous fibers (typically glass) embedded in a plastic matrix (such as a thermosetting polyester resin). The matrix serves to protect the fibers and provides for transfer of stress from the bar surface to the interior fibers. FRP bars are typically made by a process known as pultrusion (ASTM D 3918). In the pultrusion process, the continuous fibers are wetted with uncured resin and pulled through a die to form the desired cross section. After the bar has passed through the die, additional processes are used to impart a deformation pattern to the bar surface to enhance bonding when used as reinforcement in concrete. The resin is then allowed to crosslink.

The mechanical properties of FRP bars are influenced by the properties of the fibers and the matrix, the volume fractions of fibers and matrix, and the efficiency of stress transfer from the bar surface to interior fibers. The mixtures rule is often used to estimate the mechanical properties of composites, such as FRP bars:

$$P_{frp} = P_f v_f + P_m v_m \quad (1)$$

where P_{frp} = mechanical property of the FRP bar; P_f = mechanical property of the fibers; v_f = fiber volume fraction; P_m = mechanical property of the matrix; and v_m = matrix volume fraction. However, Noritake et al. (1993) have noted that when bars are formed using multiple bundles of fibers impregnated with resin, the tensile strength is generally lower than the theoretical strength. Presumably, not all fibers are effective in resisting the applied stress, and defects in the fibers reduce their strengths.

There are a variety of commercially available FRP bars for concrete reinforcement. They differ in terms of cross-sectional dimensions, composition, and surface deformation patterns. To facilitate the use of these products, it is necessary to develop standard specifications and test methods. The principal mechanical properties that need to be specified include tensile strength, modulus of elasticity, and development length. Other properties may include shear strength perpendicular to (dowel action) and parallel to (in-plane) the fibers.

FRP bars cannot be tested in tension using the same techniques that are used for steel bars. If a FRP bar is loaded using traditional wedge-shaped frictional grips, the combination of high compressive stresses and mechanical damage caused by the serrations on the wedge surfaces will lead to premature failure to the grip zone ("State-of-the-art" 1996). There is a need to develop test methods for reliable measurement of tensile strength and other mechanical properties. ASTM Subcommittee D20.18 on Reinforced Thermosetting Plastics is in the process of developing such standards. Some of the issues that have to be resolved related to tensile testing include selecting acceptable methods for introducing the tensile force into the bar and defining acceptable specimen dimensions.

For steel reinforcing bars, the modulus of elasticity can be assumed to be the same for bars from different producers. For FRP bars, the elastic modulus will depend on the materials used, the volume fractions of the materials, and the details of the production process. Since manufacturers use different materials, proportions, and processing methods, it will be necessary to measure the elastic modulus of these products. Traditionally, the elastic modulus has been obtained from the linear portion of the stress-strain curve from a tensile test.

---

[a]Contribution of the National Institute of Standards and Technology; not subject to copyright in the United States.

[1]Prof., Universidade Federal Fluminense, Niterói, Rio de Janeiro, Brazil.

[2]Leader, Struct. Evaluation Group, Struct. Div., National Institute of Standards and Technology, Gaithersburg, MD 20899.

Note. Discussion open until July 1, 1998. To extend the closing date one month, a written request must be filed with the ASCE Manager of Journals. The manuscript for this paper was submitted for review and possible publication on June 2, 1997. This paper is part of the ***Journal of Composites for Construction***, Vol. 2, No. 1, February, 1998. ©ASCE, ISSN 1090-0268/98/0001-0017–0027/$4.00 + $.50 per page. Paper No. 15887.

Standard practices are needed for bonding electrical resistance strain gages to FRP bars to ensure that bars are not damaged during gage installation. This is especially important because of the different surface textures and deformation patterns of the available bars. Electrical extensometers can be used, but they need to be properly designed to accommodate the different types of bars. An alternative approach is to measure the dynamic modulus of elasticity using stress-wave propagation methods, such as ultrasonic pulse velocity (ASTM C 597) or resonant frequency (ASTM C 215).

The study reported in this paper was undertaken to develop information to support the development of standard test methods for FRP bars. The specific objectives of this initial effort are as follows:

- Develop a simple, low-cost, and effective system for gripping FRP bars in tension.
- Examine the influence of specimen free-length on measured tensile strength.
- Compare the values of dynamic modulus of elasticity obtained from stress-wave methods with the values from tensile tests.

RESEARCH SIGNIFICANCE

The study reported in this paper adds to the body of knowledge to support the development of standard test methods for FRP reinforcing bars. This study led to the development of a simple technique for gripping FRP bars, investigated the effect of specimen free-length on measured tensile strength, and demonstrated the feasibility of using nondestructive test methods to estimate the modulus of elasticity.

BACKGROUND

End Grip Systems

ASTM D 3916 provides a procedure for performing tensile tests of pultruded smooth FRP bars with diameters ranging from 3.2–25.4 mm. The standard specifies reusable aluminum tab grip adapters to permit clamping the FRP bars in testing machines using ordinary split-wedge friction grips. Fig. 1 shows the configuration of these tabs, and Table 1 gives the key dimensions. Basically, the tabs have semicircular grooves of the same diameter as the bar to be tested. The two plates are placed around the bar and clamped together by the wedge grips of the testing machine. To increase friction, the semicircular grooves are sandblasted with 150-μm (#100 mesh) carbide grit. The minimum gripping lengths of the tabs vary from 8–16 times the bar diameter. The free-length is the length of the test specimen between the tab adapters. The values in the last column of Table 1 show the free-lengths of the specimens divided by the bar diameters. These ratios are based on the specified minimum specimen lengths and the minimum length of the tab adapters. The free-length-to-diameter ratios are not constant and vary from 30 to more than 60, depending on bar size. Unfortunately, these tab adapters can only be used with smooth round bars and would be inappropriate for FRP reinforcing bars with uneven surfaces.

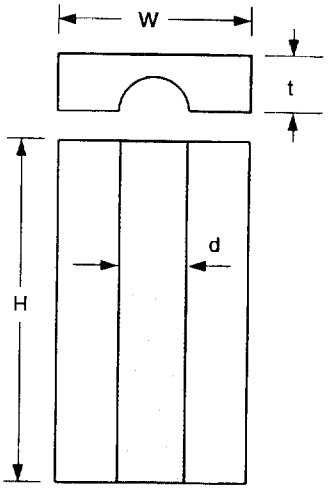

FIG. 1. Tab Grip Adapters in ASTM D 3916 for Gripping Smooth FRP Bars in Tensile Tests

Faza and GangaRao (1993) performed a review of available literature and concluded that there were no simple, reusable gripping systems for use with FRP reinforcing bars. They developed sand grips similar to the tab grip adapters in ASTM D 3916. The plates are 178 mm long, 76 mm wide, and 19 mm thick. To accommodate the deformed surfaces of the FRP bars, the semicircular grooves are 3 mm larger than the nominal bar diameter. The grooves are coated with an epoxy-sand mixture, and fine wet sand fills the remaining irregular gap between the bar and the grooves. A top plate is used to hold the tabs together while they are being placed into the jaws of the testing machine.

A variety of gripping systems have been developed to provide anchorage for the ends of FRP prestressing tendons (Nanni et al. 1996). Some of these can be used as end grips for tensile strength testing of FRP reinforcing bars. Bakis et al. (1996) used a potted grip system, as shown in Fig. 2(a), for carrying out tensile tests of FRP bars. The bar ends are rubbed with fine sandpaper and cleaned with acetone in preparation for embedment into conical end anchors. Prior to filling the cone with epoxy, fine silica sand is placed inside the cone to maintain the proper position of the bar. A rubber washer is glued to the small end of the cone to prevent uncured epoxy from leaking out of the anchor. The embedment length of the bar into the cone is 10 times the bar diameter. The bar is loaded in tension as if to measure pullout strength. This approach eliminates the high lateral compressive force in the grip region. A similar technique was developed by Holte et al.

TABLE 1. Tab Grip Adapter (TGA) and Specimen Dimensions According to ASTM D 3916-94 (See Fig. 1)

d bar diameter (mm) (1)	TGA groove diameter (mm)[a] (2)	TGA minimum width (mm) (3)	TGA thickness (mm) (4)	TGA minimum length (mm) (5)	Specimen minimum length (mm) (6)	*L* specimen free length (mm) (7)	Minimum *L*/*d* (8)
3.2	3.2	25	4	50	305	205	64
6.4	6.4	25	6.4	50	457	357	56
12.7	12.7	50	19	152	914	610	48
19.0	19.0	57	19	152	1,070	766	40
22.2	22.2	64	19	178	1,170	814	37
25.4	25.4	67	19	229	1,220	762	30

[a]Tolerance is +0.2–0.0 mm.
[b]Based on minimum lengths of TGA and specimen.

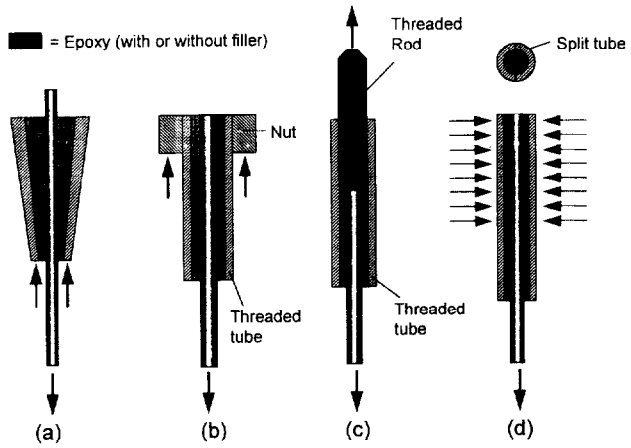

FIG. 2. Tensile Test Fittings for FRP Bars Used by Various Researchers

(1993) as anchorages for FRP prestressing tendons. In this case, the cone was machined to a parabolic profile (instead of straight) to reduce the interfacial shearing stress where the bar enters the anchor. Tensile tests with the parabolic anchors resulted in failures within the free-length and measured strengths were higher than reported by the manufacturers of the FRP rods.

Fig. 2(b) shows another potential gripping system. The ends of the bars are embedded into metal tubes with external threads (Erki and Rizkalla 1993). A collar or special nut is screwed onto each end of the tube. Load is transferred to the tubes using a special loading system, such as a center hole jack, or by modifications to the cross heads of a testing machine. This system also avoids lateral compressive force on the gripped ends of the FRP bar.

Rahman et al. (1993) used the gripping system shown in Fig. 2(c). Epoxy resin is used to embed the bar end into an internally threaded tube. The embedment length is 10 times the bar diameter. A threaded rod is used to connect the tube to the testing machine loading system. The three systems shown in Figs. 2(a–c) are similar in that the tensile force is transferred from the tube to the FRP bars by shearing stresses in the epoxy mortar. Sufficient embedment is required to ensure that the bar does not pull out from the tube.

Researchers at West Virginia University have been using another system for gripping the ends of FRP bars in tensile tests, as shown in Fig. 2(d). A 203-mm-long steel tube, with an internal diameter equal to the diameter of the FRP bar, is cut lengthwise into two pieces. The inner surfaces of the split tubes are roughened by sand blasting and coated with epoxy adhesive. The tubes are then clamped against the FRP bar until the epoxy is cured. The tensile test is carried out by gripping the tubes in the wedge grips of the testing machine. A minimum specimen length of 1219 mm is used, independent of bar diameter. This system differs from the previous ones in that compressive stresses are applied to the ends of the bar, but the tubes distribute the stresses so that they are not concentrated at high points on the bar.

In summary, several gripping systems have been proposed to enable tensile testing of FRP bars and avoid premature failures in the grip zones. The majority of them involve embedding the ends of the bar into tubes filled with a matrix, such as epoxy mortar. For such systems, it is not necessary to apply compressive clamping forces directly to the ends of the bar. Researchers tend to favor systems they have developed, and no system has been widely adopted. In addition, there does not seem to be consensus on the free-length that should be used in tensile tests.

Dynamic Modulus of Elasticity

As mentioned in the introduction, an objective of this study was to compare the values of modulus of elasticity obtained from tensile stress-strain curves with the values obtained from nondestructive tests based on stress-wave propagation. The latter is usually called the dynamic modulus of elasticity. The two methods that were studied were adapted from ASTM standards for nondestructive testing of concrete. They are the ultrasonic pulse velocity method (ASTM C 597) and the resonant frequency method (ASTM C 215).

In the ultrasonic pulse velocity test, one measures the time taken by a pulse of ultrasonic vibrations to travel through a test object. The pulse is generated by a piezoelectric transducer coupled to one side of the object, and the pulse is received by a similarly coupled transducer on the opposite side of the object. (A viscous material, such as a jelly or grease, is commonly used as a coupling agent to ensure that the vibrational energy enters the test object and that it can be detected by the receiving transducer.) An electronic timing device is used to measure and display the pulse travel time, and most devices display the travel time to the nearest 0.1 μs. The pulse velocity is calculated by dividing the distance between the transducers (D) by the measured travel time (Δt):

$$V_p = \frac{D}{\Delta t} \tag{2}$$

The speed, V_p, of compressional vibrations through an elastic solid is related to the density, ρ, modulus of elasticity, E, and Poisson's ratio, ν, as follows (Timoshenko and Goodier 1970, p. 488):

$$V_p = \sqrt{\frac{E(1-\nu)}{\rho(1-2\nu)(1+\nu)}} = \sqrt{\frac{E}{\rho}k} \tag{3}$$

By combining (2) and (3), one obtains the following relationship to estimate the dynamic Young's modulus of elasticity based on the measured time for an ultrasonic pulse to travel a known distance:

$$E_{upv} = \frac{\rho}{k}\left(\frac{D}{\Delta t}\right)^2 \tag{4}$$

Thus it is necessary to know the density and Poisson's ratio of the FRP bar to calculate its dynamic modulus, E_{upv}, from the measured pulse travel time. Benmokrane et al. (1995) reported values of Poisson's ratio for glass fibers ranging from 0.20–0.22 and values for epoxy matrix ranging from 0.20–0.33. The design manual from a manufacturer of glass FRP products made of vinyl ester matrix gives a value of 0.20. In this exploratory study, Possion's ratio for the FRP reinforcing bars was assumed to be 0.22. Fig. 3 shows the variation in the dynamic

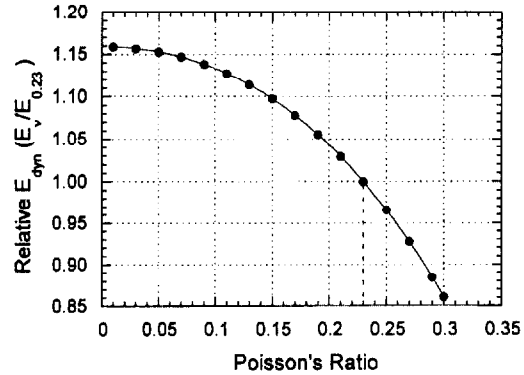

FIG. 3. Effect of Poisson's Ratio on Dynamic Modulus of Elasticity Computed from Pulse Velocity

modulus calculated from pulse velocity for different assumed values of Poisson's ratio. It is seen that a change in Poisson's ratio from 0.20 to 0.25 results in about a 10% change in the computed dynamic modulus.

The dynamic Young's modulus of elasticity of a bar can also be determined from measuring its longitudinal resonant frequency. The longitudinal resonant frequency can be obtained by fixing an accelerometer to one end of a bar specimen and tapping the other end with a small hammer. This procedure is termed impact resonance in ASTM C 215, which is one of many test methods for this purpose. (The writers chose to use ASTM C 215 because of their familiarity with this particular standard.) The output of the accelerometer is recorded by a digital frequency analyzer, and the fundamental longitudinal resonant frequency is obtained from an analysis of the frequency components in the accelerometer signal. The compressional wave speed, V_b, in the bar is related to the fundamental longitudinal resonant frequency, f_L, and the length of the bar, l, as follows (Spinner et al. 1960):

$$V_b = 2f_L l \tag{5}$$

For a long, slender rod, the wave speed is related to the dynamic Young's modulus of elasticity, E_{dyn}, and density, ρ, according to the following (Timoshenko and Goodier 1970, p. 493):

$$V_b = \sqrt{\frac{E_{dyn}}{\rho}} \tag{6}$$

This speed is often referred to as the "bar velocity" and has been derived for an infinitely long bar. However, for Poisson's ratio between 0.25 and 0.35, (6) provides an approximation that is within 0.3% of the true longitudinal wave speed for round bars with length-to-diameter ratios greater than 5 [see Spinner et al. (1960) for correction factor]. It is for this reason that test methods based on measuring the longitudinal resonant frequencies define a slender rod as a "specimen whose ratio of length to minimum cross-sectional dimension is at least 5 and preferably in the range of 20 to 25" (ASTM C 1259).

By combining (5) and (6), one obtains the following relationship for calculating the dynamic elastic modulus from the longitudinal resonant frequency:

$$E_{dyn} = 4l^2 f_L^2 \rho \tag{7}$$

In this case, no assumption is needed for Poisson's ratio.

EXPERIMENTAL PROGRAM

Gripping System

Based on the review of previous research, it was decided to explore a system based on embedding the ends of a bar into metal tubes and rely on shearing stress in the matrix to transfer the tensile force to the bar. In addition, it was desired to develop a low-cost system that would be simple to use with existing tensile testing machines. It was, therefore, necessary to select a suitable matrix material and a simple method to place the bar into tension.

The first candidate matrix material was epoxy resin, since other researchers have shown this to be suitable. Trials were carried out with 100% epoxy and epoxy mixed with fine sand. A drawback was the large volume of epoxy needed to fill the gaps between the bars and the tubes. In addition, the operation was messy and cleanup was time consuming. Therefore, it was decided to abandon epoxy resin and investigate a water-based cementitious system. Previous work showed that it is possible to couple FRP prestressing tendons using metal tubes filled with expansive cement (Khin et al. 1996; Lees et al. 1995).

After performing trial tests with several candidate materials, the authors decided to use a mortar matrix made with a high-strength gypsum cement (such as is used for capping concrete cylinders prior to compressive strength tests). The gypsum cement mortar offered the following benefits:

- It could be made with a fluid consistency so that it could be poured into the tube and consolidated without vibration.
- The setting time was long enough so that it was not necessary to rush the process of filling the tubes.
- High strength was obtained within several hours.
- The materials are inexpensive.
- Cleanup was very easy.

Washed and dried concrete sand passing a 850-μm (#20) sieve was used for the mortar. The sand reduced the amount of required cement, which in turn controlled the temperature rise and minimized shrinkage cracking. The sand also increased the frictional shear resistance of the matrix material. The mixture proportions were chosen to permit the fresh mortar to flow into the space between the FRP bar and metal tube without using vibration for consolidation. The proportions by mass were 1.0 part high-strength gypsum cement, 0.3 parts sand, and 0.3 parts water. Cold water was used to extend the setting time to assure that adequate workability was maintained during the time needed to prepare five specimens. The 50-mm cube strength of the mortar at 2 h was about 40 MPa.

The next step was to determine the embedment length to ensure that the FRP bar would not pull out of the mortar. An expeditious study led to a minimum embedment length of 15 times the bar diameter.

Finally, it was necessary to establish the method for loading the metal tube surrounding the end of the bar. The initial approach was to use a pullout arrangement in which the tubes bear on plates supported by the testing machine crossheads [Fig. 4(a)]. First, thin-walled aluminum tubes were used. During tensile testing, the tubes experienced local-buckling failure at the bearing end. Next, a steel pipe was tried (the type used for gas piping). In this case, there was an overall buckling failure of the pipe, analogous to an axially loaded flagpole (fixed-free end conditions). Finally, a steel pipe with a thicker wall was tried and found to be successful. The FRP bar failed in tension within the free-length between the tubes. At this point, the pullout method of loading was evaluated critically, and the following observations were made:

- Special hardware would be required to modify a typical tensile testing machine, adding to the cost of performing tests.

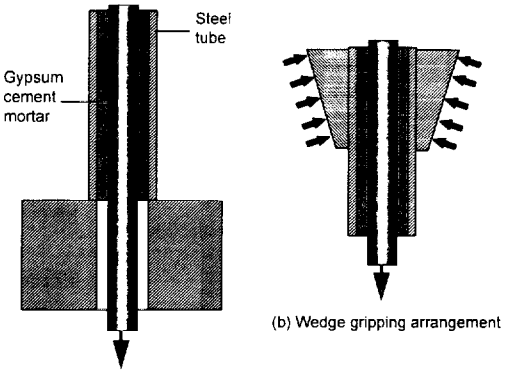

FIG. 4. Loading Schemes Used in Exploratory Study: (a) Pullout Arrangement in which Metal Tube Bears on Testing Machine Crosshead; (b) Loading through Ordinary Wedge Grip System

- The tubes would have to have sufficient size to prevent buckling failure, and this would lead to waste of material since the tubes could not be reused.
- The bar would have to be carefully centered in the tube to prevent bending of the tube.
- Care would be necessary to assure that the bearing faces of the tubes were flat, perpendicular to the bar, and parallel to each other.

Because of these requirements, it was concluded that the pullout type of loading is not practicable for routine laboratory testing. Therefore, the authors investigated an alternative method of gripping the metal tubes in the wedge grips of the testing machine, as shown in Fig. 4(b). There was concern that the transverse compressive stress, introduced by the grips, might damage the FRP bar or disrupt the embedment of the bar in the mortar. These concerns proved to be unfounded, as trial tests were successful. Therefore, this loading method was used for the remainder of the study. The metal tubes were cut from thin-walled (1.1-mm-thick), steel, electrical conduit with an outside diameter of 23.4 mm. The tube lengths are given in Fig. 5.

The procedure adopted for preparing the FRP bars for tensile tests is as follows. The tubes were cut using a metal saw without cutting fluid. The ends of the bars and the insides of the tubes were wiped with a clean cloth to remove any loose materials. Typically, five bars were prepared at a time. One end was embedded into a tube, and about 1 h later, the other end was embedded. To prepare for placing the mortar matrix, the end of each bar was positioned so that it was approximately concentric with the tube. A strip of tape was wrapped around the tube and bar, as shown in Fig. 5(a). The tape served to hold the tube in position and to contain the mortar. The tubes were clamped to a jig to hold them vertical, and the bars were aligned so that they were parallel to the tubes. Note in Fig. 5 that the tubes extended about 10 mm beyond the ends of the bars. This was done to facilitate filling the tube with

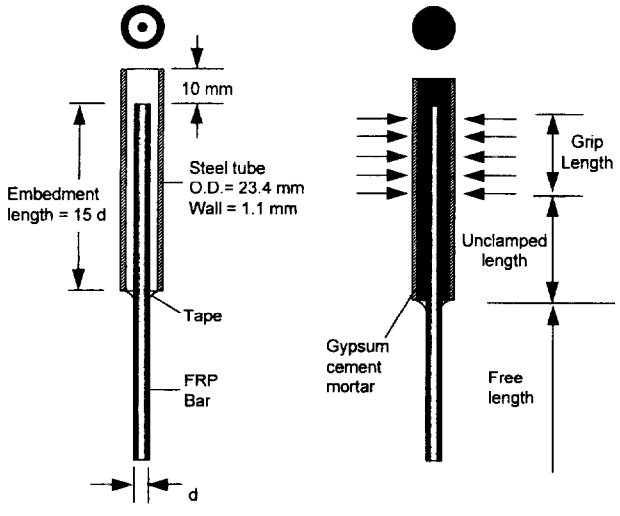

(a) Tube positioned on end of bar prior to filling with mortar

(b) Mortar-filled tube placed in wedge grips of testing machine

Bar Diameter (mm)	Embedment Length (mm)	Tube Length (mm)	Grip Length (mm)	Unclamped Length mm	Unclamped Length/ Bar Diameter
10.3	150	160	110	40	4
12.7	200	210	110	90	7
14.4	220	230	110	110	7.5

FIG. 5. Gripping System and Dimensions Adopted for Preparing Ends of FRP Bars for Tensile Tests

fresh mortar. A batch of the high-strength gypsum mortar was mixed by hand and poured into the space between the bar and tube. The next day, the bars were tested in tension. Typically, five replicate specimens were tested for each condition being investigated. This number is suggested by ASTM D 3916.

Tensile Tests

Tensile tests were carried out using a 270-kN-capacity, manually operated, universal testing machine. The specimens were loaded at a rate of approximately 250 MPa/min. Bar elongation was measured using an LVDT-based, clip-on extensometer with a 50.8-mm gage length. A pressure transducer was added to the hydraulic weighing system of the testing machine to permit recording load data. A displacement sensor was used to monitor the movement of the testing machine table. The extensometer, pressure transducer, and displacement sensor were connected to a digital data acquisition system, and the three channels were read twice per second. The extensometer was removed from the bar at about 70% of the expected ultimate load to avoid damage. A test was continued until the specimen fractured and there was a sudden drop in the load. Only results in which failures occurred in the free-length of the specimen were considered valid for the determination of the tensile strength.

The raw load-displacement data were stored on disk and later converted to engineering units using previously established calibration relationships. Fig. 6 shows examples of the data recorded during a typical tensile test. Fig. 6(a) shows table position versus time. These data can be used to establish the approximate rate of stretching of the specimen. Fig. 6(b) shows the tensile stress versus table position. The shape of this curve is similar to the stress-strain curve, and it shows that fracture occurs abruptly without prior warning. Fig. 6(c) shows tensile stress versus strain. The erratic nature of the data in Fig. 6(c) is due, in part, to the limited resolution of the data acquisition system and the low sensitivity of the extensometer. Linear regression analysis was used to find the best-fit line to the points in the linear portion of the stress-strain plot, and the slope of the line is the static modulus of elasticity.

Effective Bar Diameter

Three types of commercially available FRP reinforcing bars and two types of smooth bars were tested. All pultruded bars are composed of E-glass fibers embedded in a vinyl ester or polyester matrix. The descriptions and nominal diameters (according to the manufacturer) of the bars are as follows:

- SC = 9 mm nominal diameter, wrapped with a fiber bundle in a spiral pattern at a pitch of about 30 mm, and sand coated to increase pullout resistance
- SW = 12.7 mm nominal diameter, wrapped with a fiber bundle in a spiral pattern at a pitch of about 20 mm
- RB = 15 mm nominal diameter, with a ribbed surface similar to steel reinforcing bars
- SMQ = 12.7 mm, smooth square bar
- SMR = 12.7 mm, smooth round bar

To calculate the tensile strength and the modulus of elasticity, the diameter of the bar must be known. ASTM D 3916 specifies measuring the diameter of a smooth bar with a micrometer at "several points along its length" and noting the minimum and average values. This approach would be impracticable for deformed FRP bars because of the great variation in cross-sectional dimensions, or the presence of ribs. A better approach would be to calculate the average diameter from the mass, length, and density of a representative portion of the bar. The density can be determined by measuring the

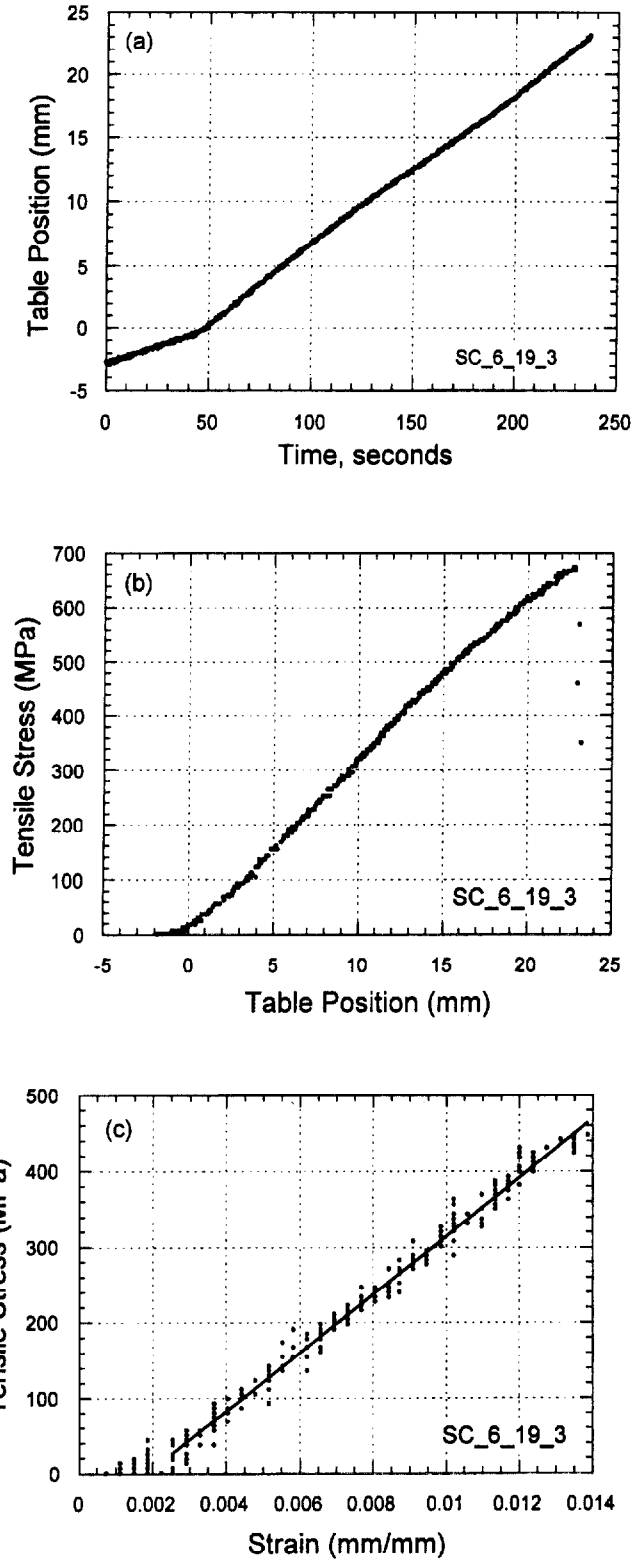

FIG. 6. Example of Data Recorded in Tensile Tests: (a) Table Position versus Time; (b) Tensile Stress versus Table Position; (c) Stress versus Strain

volume of water displaced by the bar using a pycnometer. A study was done to determine the minimum length of bar that should be used to obtain a representative density. A comparison of densities measured using specimens of different lengths showed that, for the bars in this study, 200 mm was sufficient for obtaining a representative measure of density.

Another study was done to gain an understanding of the inherent variability in determining bar diameter and density

TABLE 2. Results of Four Replicate Determinations of Bar Diameter and Density Using Pycnometer Method

Bar (1)	Average diameter (mm) (2)	Standard deviation (mm) (3)	Average density (kg/m³) (4)	Standard deviation (kg/m³) (5)
(*a*) Spiral wound bars				
SW1	14.05	0.09	1,950	22
SW2	14.06	0.04	1,949	10
SW3	14.13	0.02	1,938	5
SW4	13.93	0.02	1,960	6
SW5	14.12	0.06	1,930	16
[Average]	14.06	0.05	1,945	12
[Standard deviation of average]	0.08	—	12	—
(*b*) Sand coated bars				
SC1	10.15	0.17	2,038	69
SC2	10.03	0.19	2,072	79
SC3	9.95	0.19	2,072	79
SC4	10.21	0.19	2,007	74
SC5	9.89	0.20	2,077	85
Average	10.05	0.19	2,053	77
[Standard deviation of average]	0.13	—	30	—

from the pycnometer method. Five 200-mm-long samples of SC and SW bars were subjected to 4 replicate determinations of density and bar diameter. The results are shown in Table 2. For the SW bar, an electronic balance reading to the nearest 0.01 g was used, while a balance reading to the nearest 1 g was used for the SC bars. This accounts for the higher within-test variability of the four replicate determinations for the SC bars. For comparison, 10 replicate diameters were measured with a micrometer, reading to the nearest 0.01 mm. The average values from the direct measurements were 14.3 and 10.4 mm with coefficients of variation of 4.7 and 2.5% for the SW and SC bars, respectively.

Dynamic Modulus of Elasticity

The impact resonance procedure in ASTM C 215 was adapted to determine the dynamic elastic modulus of the FRP bars from the measured longitudinal resonant frequencies. A compression stress-wave was introduced in the bar by striking one end with a steel hammer. A small hammer was used to produce a short duration pulse that contained frequencies greater than the resonant frequency to be measured. (A smaller hammer has to be used for shorter specimens.) An accelerometer was attached to the opposite end of the bar with a soft wax. The accelerometer was connected to a waveform analyzer and data were recorded at sampling frequencies of 20 kHz or greater, depending on the specimen length. The waveform analyzer displayed the amplitude spectrum of the accelerometer signal, from which the high-amplitude frequency corresponding to the resonant frequency was determined. The bar was supported on a sponge rubber pad. The impacts were repeated three times, and in most cases the same digital value of resonant frequency was obtained from the replicate impacts. The average density previously established for each type of bar was used to calculate the dynamic modulus of elasticity according to (7). This elastic modulus is identified as E_{impact} in the rest of the paper.

Ultrasonic pulse velocity (UVP) tests were carried out on the same specimens used for the impact resonance test. A silicone grease was used to couple the 54-kHz transducers to the ends of the bar. The travel time was measured to the nearest 0.1 μs. The dynamic modulus of elasticity was computed according to (4) with a value of $k = 1.14$, which corresponds to

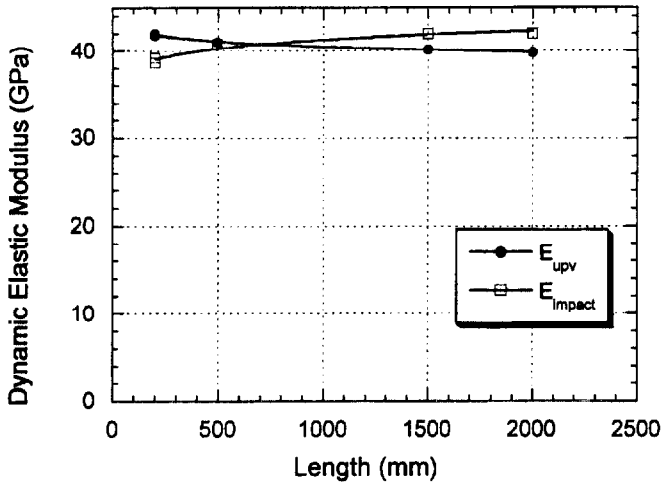

FIG. 7. Effect of Specimen Length on Computed Dynamic Modulus of Elasticity by Ultrasonic Pulse Velocity and Resonant Frequency (RB Type Bar)

a Poisson's ratio of 0.22. This dynamic modulus of elasticity is identified as E_{upv} in the rest of the paper.

In the impact-resonance test, the longitudinal resonant frequency increases as the specimen length decreases. When a digital spectrum analyzer is used to determine the value of the resonant frequency, the frequency resolution is fixed by record length (the duration of the recorded accelerometer signal). If the frequency resolution is constant, more accurate estimates of the dynamic elastic modulus would result if shorter specimens are used, provided the specimen is long enough to be representative of the entire bar and satisfy the definition of a slender bar. On the other hand, in the pulse velocity test, the travel time is read to one same resolution for all bar lengths. In this case, more accurate estimates of the dynamic elastic modulus would be obtained with longer specimens. An exploratory study was done to compare the computed values of the dynamic elastic modulus for different specimen lengths. The ribbed bars with high fiber content (61% by volume) were used for this comparison. The results are shown in Fig. 7. It was found that the computed elastic modulus values increased with specimen length for the impact-resonance procedure, while they decreased for the pulse velocity procedure. An explanation for this phenomenon is beyond the scope of this exploratory study. However, additional experiments should be designed to understand this behavior so that specimen length can be specified rationally in a future standard test method.

RESULTS AND COMMENT

Tensile Strength

Variability

The main objectives of the tensile test study were to examine the variability of results with the gripping system that was adopted and to examine whether the free-length of the test specimen affects the results. Tests were conducted using free-length-to-bar-diameter ratios (L/d) varying between 40 and 70. The bar types included: sand coated (SC), spiral wound (SW), smooth round (SMR), and smooth square (SMQ). Five replicate specimens were tested for each case. Table 3 shows the test results. Due to time constraints, not all L/d values were used for each bar type. Table 4 lists the mean strengths and their standard deviations. No attempt was made to determine the effective diameter of each bar. Instead, tensile strengths were calculated using average effective diameters (or side length for the square bars) determined from randomly chosen bars (Table 2). Thus the variabilities in Table 4 should be viewed as those for the ultimate bar forces, which are of direct value in assessing the flexural capacities of reinforced members.

TABLE 3. Tensile Strength and Static Modulus of Elasticity of FRP Bars

ID[a] (1)	L/d (2)	TS (MPa) (3)	E_{static} (GPa) (4)
(*a*) Sand coated bars			
SC10620	70	697.9	39.0
SC20620	70	681.2	37.9
SC30620	70	582.8	35.5
SC10530	70	751.4	38.9
SC20530	70	739.6	38.0
SC10607	60	736.6	38.6
SC20607	60	608.1	33.3
SC50607	60	604.9	41.0
SC30619	60	678.5	38.5
SC50619	60	615.1	36.5
SC40620	50	681.2	37.9
SC50620	50	582.8	36.0
SC60620	50	600.6	35.3
SC30530	50	704.3	36.0
SC40530	50	678.6	38.0
SC10515	40	620.2	34.9
SC20515	40	725.7	39.1
SC30515	40	704.8	40.6
SC50530	40	591.3	36.6
SC60530	40	723.0	36.5
(*b*) Spiral wound bars			
SW20515	40	601.8	29.8
SW30515	40	583.5	34.8
SW10619	40	698.7	35.6
SW20619	40	700.6	33.4
SW30619	40	686.3	32.8
(*c*) Smooth round bars			
SMR20620	50	816.2	46.5
SMR10619	50	786.9	44.5
SMR10530	50	865.4	45.7
SMR20530	50	793.2	45.3
SMR30530	50	836.4	45.5
SMR10607	60	827.9	45.4
SMR20607	60	811.3	44.5
SMR30607	60	827.9	43.1
SMR40607	60	812.7	45.0
SMR10620	60	856.2	45.5
(*d*) Smooth square bars			
SMQ4b70	70	700.0	46.3
SMQ1b70	70	725.8	42.2
SMQ2b70	70	715.9	45.3
SMQ3b70	70	816.1	46.9
SMQ5b70	70	780.0	47.2
SMQ6a60	60	704.4	42.6
SMQ160	60	821.5	45.1
SMQ260	60	—[b]	42.9
SMQ7a60	60	788.3	47.4
SMQ360	60	787.2	46.1
SMQ450	50	813.8	44.7
SMQ550	50	796.9	42.3
SMQ7b50	50	728.9	46.9
SMQ6b50	50	713.0	41.2
SMQ3b50	50	811.3	—
SMQ1a40	40	735.5	43.2
SMQ5a40	40	795.7	46.3
SMQ2a40	40	768.6	47.8
SMQ4a40	40	770.0	44.7
SMQ3a40	40	756.3	—

[a]Numbers indicate replicate numbers and test dates, except for the SMQ bars where the numbers indicate replicate number and L/d values.
[b]Bar slipped from tube.

TABLE 4. Average, Standard Deviation, and Coefficient of Variation of Tensile Strength Results

L/d (1)	Number of tests (2)	Mean tensile strength (MPa) (3)	Standard deviation (MPa) (4)	Coefficient of variation (%) (5)
(a) Sand coated bars				
70	5	690.6	62.8	9.1
60	5	648.6	54.1	8.3
50	5	646.5	57.7	8.9
40	5	673.0	66.8	9.9
(b) Spiral wound bars				
40	5	654.2	56.8	8.7
(c) Smooth round bars				
60	5	827.2	18.1	2.2
50	5	819.6	32.2	3.9
(d) Smooth square bars				
70	5	747.5	48.7	6.5
60	4	775.3	49.9	6.4
50	5	772.0	48.1	6.2
40	5	764.6	20.9	2.7

Table 4 shows that the tensile strength of the deformed bars (SC and SW) appear to have higher within-test variability than the smooth bars. The coefficient of variation for the tensile strength of the deformed bars is about 9%. Such a high variability means that the average strength of five specimens will not provide a reliable estimate of the true mean strength. The relationship in ASTM E 122 can be used to calculate the likely relative error, e, at the 0.05 risk level, between the true mean strength and the mean strength obtained from n test specimens.

$$e = \pm\frac{1.96CV}{\sqrt{n}} \tag{8}$$

If a coefficient of variation of 9% is substituted for CV and 5 for n, the calculated relative error is ±7.9%. If it is desired to reduce the error to only ±2%, over 70 bars would have to be tested for a risk level of 0.05!

L/d Effect

Another objective was to investigate the effect, if any, of the *L/d* value. Figs. 8(a) and 8(b) show the individual test results for the sand coated and smooth square bars. Analysis of variance (ANOVA) was used to determine whether there were any differences in the mean strengths due to *L/d*. The results of the ANOVA showed that there were no statistically significant differences due to *L/d* for either type of bar. Thus it is concluded that, based on 5 replicate tests, an *L/d* value in the range of 40–70 has no statistically significant effect on the mean strength. If there really is an effect, it would be necessary to test more than five bars at each *L/d* value to detect the magnitude of the effect.

Strength versus Static Elastic Modulus

As shown in Table 3, values of static modulus of elasticity were obtained from the linear portions of the stress-strain curves. Fig. 9 shows the static elastic modulus plotted as a function of the tensile strength. As expected, there is some correlation between elastic modulus and tensile strength. The reason for the correlation is obvious: as the fiber content increases, the mixtures rule [(1)] predicts increases in both strength and stiffness. Fig. 9 also shows that the relative scatter of the elastic modulus values for each bar type is less than the relative scatter of the tensile strength. This is also not surprising. The tensile strength is expected to be affected by imperfections in a composite material, while the elastic modulus is expected to be less sensitive to defects.

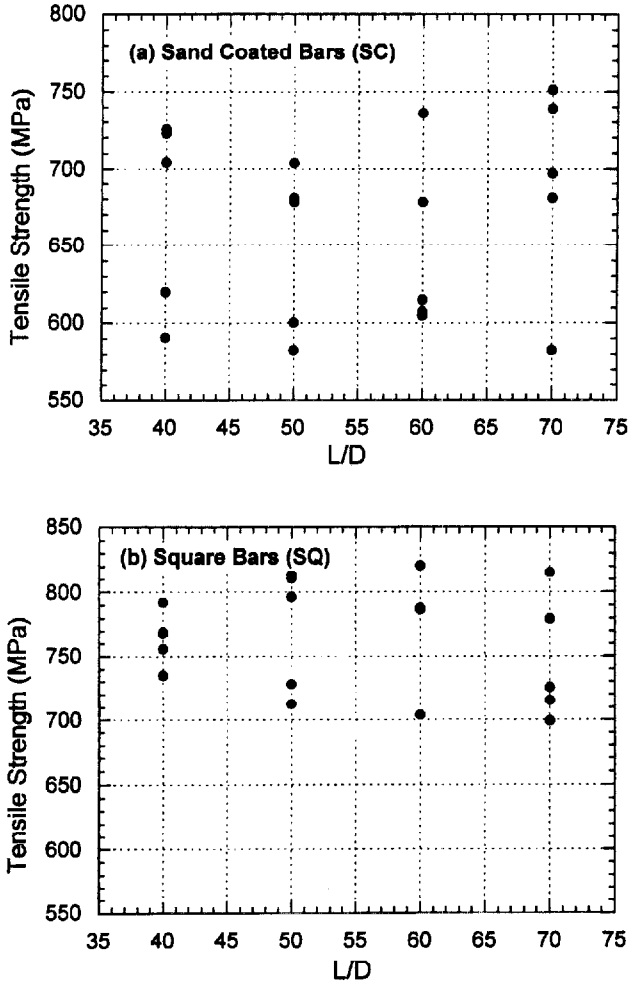

FIG. 8. Tensile Test Results for Sand-Coated and Square Bars for Different *L/D* Values

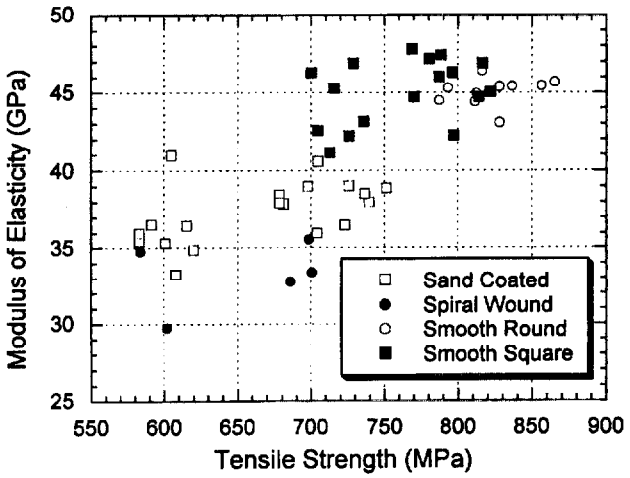

FIG. 9. Static Modulus of Elasticity versus Tensile Strength

Modulus of Elasticity

The other major objective of this study was to compare static elastic modulus values obtained from tensile stress-strain curves with the dynamic values obtained nondestructively. Table 5 shows the elastic modulus values obtained by the three methods for smooth square bars and the ribbed bars with two

TABLE 5. Static and Dynamic Modulus of Elasticity for Smooth Square and Ribbed FRP Bars

ID (1)	Length (mm) (2)	E_{static} (GPa) (3)	E_{upv} (GPa) (4)	E_{impact} (GPa) (5)
(*a*) Smooth square bar				
SMQ4B70	1,246	46.3	45.0	47.4
SMQ1B70	1,247	42.2	43.3	44.6
SMQ2B70	1,247	45.3	44.3	46.5
SMQ3B70	1,247	46.9	45.0	47.5
SMQ5B70	1,248	47.2	45.5	47.5
SMQ6A60	1,132	42.6	44.8	47.3
SMQ160	1,100	45.1	45.0	47.2
SMQ260	1,098	42.9	43.2	44.5
SMQ7A60	1,232	47.4	41.5	47.3
SMQ360	1,100	46.1	44.7	46.3
SMQ450	1,016	44.7	44.6	46.1
SMQ550	1,015	42.3	43.0	44.5
SMQ7B50	1,000	46.9	45.1	46.9
SMQ6B50	996	41.2	45.1	46.5
SMQ1A40	885	43.2	43.6	44.8
SMQ5A40	885	46.3	45.7	46.8
SMQ2A40	885	47.8	45.0	46.2
SMQ4A40	885	44.7	45.5	46.8
SMQ3A40	885	—	45.2	46.8
(*b*) High fiber volume ribbed bar				
RB-BBFC	1,184	—	40.3	42.6
RB-BBEC	1,185	41.1	40.2	41.8
RB-BBFA	1,187	38.4	40.5	41.9
RB-BBEF	1,185	41.8	40.5	42.2
RB-BBEH	1,185	41.8	40.4	41.8
RB-BBFE	1,188	—	40.7	42.0
RB-BBEG	1,186	37.4	40.5	42.3
RB-BBED	1,185	38.9	40.2	42.2
RB-BBFB	1,185	40.8	40.4	42.2
RB-BBEI	1,500	41.0	40.2	42.0
RB-BBFC	815	40.2	40.8	42.1
RB-BBEC	814	40.6	40.5	41.7
RB-BBEJ	814	42.5	40.3	42.0
RB-BBEE	812	42.7	40.9	42.4
RB-BBEH	814	42.3	41.0	41.7
RB-BBFD	808	46.6[a]	40.5	41.9
RB-BBEG	814	39.9	40.4	41.7
RB-BBED	812	39.9	40.7	41.6
RB-BBFB	809	59.1[a]	40.9	42.0
RB-BBEI	495	—	41.1	40.9
(*c*) Low fiber volume ribbed bar				
RB-BCCE	1,188	32.0	31.9	33.5
RB-BCCB	1,193	32.4	32.2	33.1
RB-BCBJ1	1,192	33.8	32.1	33.0
RB-BCCI	1,192	32.1	32.2	33.0
RB-BCBJ	1,193	33.0	32.2	33.1
RB-BCCF	1,190	32.7	31.7	33.3
RB-BCCG	1,193	32.1	31.6	33.1
RB-BCCD	1,192	33.1	32.2	33.4
RB-BCBH	1,191	47.5[a]	32.0	33.0
RB-BCCJ	1,191	34.7	32.0	33.0
RB-BCCD	813	32.4	31.9	33.2
RB-BCCB	810	—	31.9	32.9
RB-BCBI	803	36.2[a]	32.4	33.1
RB-BCCH	807	33.1	32.0	33.0
RB-BCBJ	805	33.3	32.0	33.0
RB-BCCF	807	30.4	32.1	32.8
RB-BCCG	810	32.9	31.6	32.9
RB-BCCC	802	—	32.2	33.0
RB-BCBH	803	32.4	32.4	33.1
RB-BCCI	805	31.6	32.6	33.0

[a]Results judged to be outliers on the basis of normal probability plots; not used in ANOVA.

different volume fractions of fibers (61% and 47% by volume). The individual values are plotted in Fig. 10. An examination of Fig. 10 shows two trends: (1) The elastic modulus values obtained from the tensile stress-strain curves, E_{static}, have

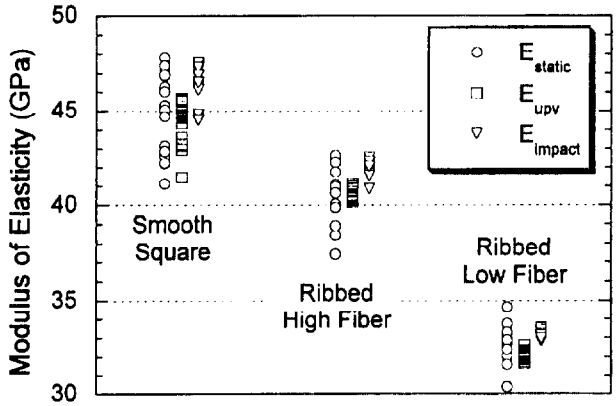

FIG. 10. Comparison of Elastic Modulus Values Obtained from Different Test Methods for Smooth Square Bars and Ribbed Bars

greater variability than the values from the nondestructive tests; and (2) the values obtained from the impact resonance procedure, E_{impact}, tend to be greater than those from the pulse velocity procedure, E_{upv}.

Table 6 shows the average values and standard deviations for the three measures of elastic modulus for the three types of bars. An ANOVA was carried out within each bar type to establish whether the differences in means shown in Table 6 are statistically significant. In addition, a post hoc test of multiple differences, using the Scheffé method, was carried out to identify which differences were statistically significantly at the 0.05 risk level. The following summarizes the results of the comparison.

1. Square smooth bars:
   - The difference between E_{static} and E_{upv} is not statistically significant.
   - The difference between E_{static} and E_{impact} is statistically significant ($p = 0.015$).
   - The difference between E_{upv} and E_{impact} is statistically significant ($p < 0.001$).
2. Ribbed high fiber bars:
   - The difference between E_{static} and E_{upv} is not statistically significant.
   - The difference between E_{static} and E_{impact} is statistically significant ($p < 0.001$).
   - The difference between E_{upv} and E_{impact} is statistically significant ($p < 0.001$).
3. Ribbed low fiber bars:
   - The difference between E_{static} and E_{upv} is statistically significant ($p = 0.010$).
   - The difference between E_{static} and E_{impact} is statistically significant ($p = 0.05$).
   - The difference between E_{upv} and E_{impact} is statistically significant ($p < 0.001$).

In general, there was closer agreement between E_{static} and E_{upv} than between E_{static} and E_{impact}. However, recall that the elastic modulus was computed from the pulse velocity by assuming a value of 0.22 for Poisson's ratio. Until further studies are carried out it can not be concluded with certainty that the pulse velocity approach provides a closer estimate of E_{static}.

While the ANOVA revealed statistically significant differences among the various measures of elastic modulus, the differences were between about 2 and 4%, which may not be of practical significance. In any case, this exploratory study confirmed the applicability of nondestructive test methods for estimating the modulus of elasticity of FRP bars. The advantages of the nondestructive methods, compared with obtaining a tensile stress-strain curve, are their simplicity and speed.

TABLE 6. Average and Standard Deviation of Modulus of Elasticity Values from Static Tensile Tests, Ultrasonic Pulse Velocity, and Impact Resonance

Bar type (1)	E_{static}			E_{upv}			E_{impact}		
	Average (GPa) (2)	Standard deviation (3)	Number of tests (4)	Average (GPa) (5)	Standard deviation (6)	Number of tests (7)	Average (GPa) (8)	Standard deviation (9)	Number of tests (10)
Square (SMQ)	45.0	2.03	19	44.5	1.10	19	46.4	1.03	19
Ribbed–high fiber (RB-BB)	40.6	1.53	15	40.5	0.27	20	41.9	0.36	20
Ribbed–low fiber (RB-BC)	32.6	0.95	16	32.0	0.24	20	33.1	0.17	20

SUMMARY AND RECOMMENDATIONS

A successful system was developed for gripping the ends of FRP bars for the purpose of performing tensile tests. The system uses inexpensive steel tubes and a high-strength gypsum cement mortar to provide an end assembly that can be grabbed by ordinary wedge grips of the testing machine. The system was successful for testing not only deformed bars but also smooth bars with round and square cross sections.

A comparison of measured tensile strengths, using five replicate tests, indicated no significant effect due to the *L/d* value of the test specimen. However, it was observed that the tensile strengths had high within-test variability, and more than five replicate tests would be necessary to discern small differences due to *L/d*.

It has been demonstrated that it is possible to measure the dynamic modulus of elasticity using established nondestructive test methods based on stress-wave propagation. The results showed good agreement between average values of static and dynamic modulus. The dynamic values had less within-test variability than the static values.

The following studies are recommended to support further the development of standards for FRP reinforcement:

- Studies should be performed to establish the within-test variability of the tensile strength of FRP bars produced by different manufacturers. This will provide a better understanding of the inherent variability of FRP reinforcement. Such information is critical for determining the number of required tests to demonstrate compliance with specifications and to establish the characteristic (or minimum) strength for design purposes.
- Studies of the effect of the *L/d* values are needed to establish conclusively whether this variable has a significant influence on measured tensile strength. More than five replicate tests, as used in this study, will probably be needed.
- Studies are needed to better understand the influence of specimen length on the dynamic elastic modulus obtained by nondestructive testing. Such information is necessary to develop a standard test method for dynamic elastic modulus.
- Due to the irregular cross-sectional dimensions of some FRP bars, the industry should consider adopting specification limits for ultimate bar force instead of ultimate stress. In flexural design, the bar force is the important variable. Such an approach would eliminate the need to measure the effective bar diameter to demonstrate compliance with strength specifications. A nominal bar diameter could be used for considerations of cover depth, development length, and bar spacing.

APPENDIX I. REFERENCES

Bakis, C. E., Nanni, A., and Terosky, J. A. (1996). "Smart, pseudo-ductile, reinforcing rods for concrete: manufacture and test." *Proc., 1st Int. Conf. on Compos. in Infrastructure, ICCI 96*, Tucson, Ariz., M. Ehsani and H. Saadatmanesh, eds., 95–108.

Benmokrane, B., Chaallal, O., and Masmoudi, R. (1995). "Glass fibre reinforced plastic (GRFP) rebars for concrete structures." *Constr. and Build. Mat.*, 9(6), 354–364.

Erki, M. A., and Rizkalla, S. H. (1993). "Anchorages for FRP reinforcement." *Concrete Int.*, 15(6), 54–59.

Faza, S., and Gangarao, H. (1993). "Glass FRP reinforcing bars for concrete." *Fiber-reinforced-plastic (FRP) reinforcement for concrete structures—properties and applications*, A. Nanni, ed., Elsevier Science Publishing Co. Inc., New York, N.Y., 167–188.

Holte, L. E., Dolam, C. W., and Schmidt, R. J. (1993). "Epoxy socketed anchors for non-metallic prestressing tendons." *Fiber-reinforced-plastic reinforcement for concrete struc.—int. symp. ACI SP-138*, A. Nanni and C. W. Dolan, eds., American Concrete Institute, Farmington Hills, Mich., 381–400.

Khin, M., Harada, T., Tokumitsu, S., and Idemitsu, T. (1996). "The anchorage mechanism for FRP tendons using highly expansive materials for anchoring." *Proc., 2nd Int. Conf. on Advanced Compos. Mat. in Bridges and Structures*, M. M. El-Badry, ed., Canadian Society for Civil Engineering, Montreal, Canada, 959–964.

Lees, J. M., and Gruffydd-Jone, B., and Burgoyne, C. J. (1995). "Expansive cement couplers: a means of pretensioning fibre-reinforced plastic tendons." *Constr. and Build. Mat.*, 9(6), 413–423.

Nanni, A., Bakis, C. E., O'Neil, E. F., and Dixon, T. O. (1996). "Short-term sustained loading of FRP tendon-anchor systems." *Constr. and Build. Mat.*, 10(46), 255–266.

Noritake, K., Kakihara, R., Kumagai, S., and Mizutani, J. (1993). "Technora, and aramid FRP rod." *Fiber-reinforced-plastic (FRP) reinforcement for concrete structures—properties and applications*, A. Nanni, ed., Elsevier Science Publishing Co. Inc., New York, N.Y., 267–290.

Rahman, A. H., Taylor, D. A., and Kingsley, C. Y. (1993). "Evaluation of FRP as reinforcement for concrete bridges." *Fiber-reinforced-plastic reinforcement for concrete struct.—int. symp., ACI SP-138*, A. Nanni and C. W. Dolan, eds., American Concrete Institute, Farmington Hills, Mich., 71–82.

Spinner, S., Reichard, T. W., and Tefft, W. E. (1960). "A comparison of experimental and theoretical relations between Young's modulus and the flexural and longitudinal resonance frequencies of uniform bars." *J. Res. of the Nat. Bureau of Standards*, 64A(2), 145–155.

Standard definitions and terminology of terms relating to reinforced plastic pultruded products; D 3918. (1996). ASTM, West Conshohocken, Pa.

Standard practice for choice of sample size to estimate a measure of quality for a lot or process; E 122. (1996). ASTM, West Conshohocken, Pa.

Standard test method for dynamic Young's modulus, shear modulus, and Poisson's ratio for advanced ceramics by impulse excitation; C1259. (1996). ASTM, West Conshohocken, Pa.

Standard test method for fundamental transverse, longitudinal, and torsional frequencies of concrete specimens; C 215. (1996). ASTM, West Conshohocken, Pa.

Standard test method for pulse velocity through concrete; C 597. (1996). ASTM, West Conshohocken, Pa.

Standard test method for tensile properties of pultruded glass-fiber-reinforced plastic rod; D 3916. (1996). ASTM, West Conshohocken, Pa.

"State-of-the-art report on fiber reinforced plastic reinforcement for concrete structures." (1996). *ACI 440R-96*, American Concrete Institute, Farmington Hills, Mich.

Timoshenko, S. P., and Goodier, J. N. (1970). *Theory of elasticity*, McGraw Hill Book Co. Inc., New York, N.Y.

APPENDIX II. NOTATION

The following symbols are used in this paper:

CV = coefficient of variation;
D = distance between transducers;

d = bar diameter;
E = modulus of elasticity;
E_{dyn} = dynamic modulus of elasticity;
E_{Impact} = modulus of elasticity from impact resonance test;
E_{static} = modulus of elasticity from tensile stress-strain curve;
E_{upv} = modulus of elasticity from pulse velocity test;
e = error between true mean of a population and mean based on a sample;
f_L = fundamental resonant frequency of the longitudinal mode;
k = factor in wave speed equation dependent on Poisson's ratio;
L = free-length of bar in tensile test;
l = length of specimen for resonant frequency test;
n = number of replicate specimens;
P_f = mechanical property of the fibers;
P_{frp} = mechanical property of the FRP bar;
P_m = mechanical property of the matrix;
V_b = wave speed for vibration of bar in the longitudinal mode;
V_p = speed of compressional wave;
v_f = fiber volume fraction;
v_m = matrix volume fraction;
Δt = travel time of ultrasonic pulse;
ν = Poisson's ratio; and
ρ = density.